

## Modern Distribution of *Thalassionema* species (Bacillariophyceae) in the Pacific Ocean

Yoshihiro Tanimura<sup>1</sup>, Chieko Shimada<sup>2</sup>, and Masao Iwai<sup>3</sup>

<sup>1</sup> Department Geology and Paleontology, Division of Paleoenvironment and Paleoecology,  
National Museum of Nature and Science, Tokyo 169–0073, Japan

<sup>2</sup> Mineral Industry Museum, Akita University, Akita; Geological Survey of Japan,  
Advanced Industrial Science and Technology (AIST), Ibaraki 305–8567, Japan

<sup>3</sup> Department of Natural Environmental Science, Faculty of Science, Kochi University, Kochi 780–8520, Japan

**Abstract** Using core-top sediment samples, we measured the modern distribution of *Thalassionema* species and their morphological types in the Pacific Ocean. Strong correlations between *Thalassionema* distributions in the sediments (*T. pseudonitzschiooides* and six morphological variants of *T. bacillare* and *T. nitzschiooides*) and the modern gyral circulation systems over sediments in the Pacific were found. Two morphological variants of *T. nitzschiooides* s. l. and *T. pseudonitzschiooides* were common in sediments under the Subpolar Gyre and under the region northwest of the Kuroshio Front in the North Pacific. One morphological type of *T. nitzschiooides* s. l. and two morphological variants of *T. bacillare* were widely distributed in the sediments under the Subtropical Gyres of the North and South Pacific and under the Equatorial Current System. Three types of *T. nitzschiooides* s. l. were primarily restricted to the sediments south of the Subtropical Convergence in the South Pacific. The Kuroshio Front that forms between the Subtropical and Subpolar Gyres and the Subtropical Convergence in the South Pacific are distinct boundaries of the distributions of *Thalassionema* species in the Pacific Ocean.

**Key words:** Modern distribution, Pacific Ocean, *Thalassionema* spp.

### Introduction

Based on the temporal and spatial distribution of foraminifers, calcareous nannofossils, radiolaria, and diatoms in Deep Sea Drilling Project (DSDP) cores, Sancetta (1978) demonstrated large changes in the latitudinal distribution of plankton provinces from the Early to Middle Miocene. Sancetta (1978) documented a widening of the Tropical province during the Early to Middle Miocene and inferred both a strong Kuroshio Current in the North Pacific and a strong subtropical convergence in the South Pacific. From analyses of changes in the fossil diatom assemblages in seven sediment cores, Sancetta and Silvestri (1986) also inferred that prior to 2.5 Ma, the modern subarctic water mass did not exist, at least in the western Pacific. Similarly, based on the biogeographical distribution of

planktonic foraminifers, Kennett *et al.* (1985) described important differences in surface water circulation systems between the Early and Late Miocene. For example, Kennett *et al.* (1985) concluded that the gyral circulation system was weakly developed in the Early Miocene, but became stronger by the Late Miocene in association with the closure of the Indonesian Seaway and the intensification of the Kuroshio Current in the Middle Miocene.

Tanimura (1999) analyzed data from sediment traps and sediment cores from the northwest Pacific and determined that: (1) three *T. nitzschiooides* varieties (*T. nitzschiooides* var. *incurvatum*, *T. nitzschiooides* var. *inflatum*, and *T. nitzschiooides* var. *parvum*) are the major floral components in waters of the Subtropical Gyre in the North Pacific, whereas *T. nitzschiooides* s. s. is relatively abundant in waters northwest of the

Kuroshio Current, (2) the proportions of the three *T. nitzschiooides* varieties relative to *T. nitzschiooides* s. s. reflect the path migrations of the current, and (3) these proportions are potentially useful tools for delineating past migrations of the Kuroshio Current. The determinations cited above, together with the inferences of evolution in plankton provinces and surface water circulation systems in the geologic past (Sancetta, 1978; Kennett *et al.*, 1985) leads us to test the idea that the evolution of a surface water circulation system in the Pacific could affect the speciation of marine plankton diatoms, particularly the varieties and morphological types of *Thalassionema* species. We investigated the modern distribution of *Thalassionema* species and the morphological types within morphological variants of the species in the uppermost layers of deep-sea cores collected from the Pacific Ocean. We discuss correlations between the distribution of these species in the sediment layers and the modern gyral circulations and current systems over sediments in the Pacific. In general, surface water circulation systems cause the formation and distribution of surface water masses in which marine diatoms are produced. The distributions of *Thalassionema* species and their morphological types were correlated with this system. Our results provide the initial step in a broader project to use down-core analysis for the reconstruction of the evolution of *Thalassionema* species in the Pacific.

Species and varieties belonging to the genus *Thalassionema* are cosmopolitan in all but the high-latitude Arctic and Antarctic seas (Hasle and Syvertsen, 1996). These species often occur in large numbers and are dominant components of the plankton diatom flora (Hasle, 1960; Simonsen, 1974). *Thalassionema* species range in age from the Eocene to Recent (Schrader, 1978; Barron, 1985; Baldauf and Monjanel, 1989; Fenner and Mikkelsen, 1990; Baldauf and Barron, 1991; Gladenkov and Barron, 1995). Diatoms in this genus are primarily heavily silicified; thus, they are abundant in pelagic and hemipelagic sediments and are dominant constituents of sediment

diatom assemblages.

Valves of *Thalassionema* species and varieties are highly variable in morphology in modern seas, and more than 18 taxa have been defined mainly from valve outlines (Grunow in Van Heurck, 1881; Peragallo, 1903; Heiden and Kolbe, 1928; Cleve-Euler, 1949; Table 1). The genus *Thalassionema* is ideal for our research purposes because of its wide distribution in modern oceans, its abundance in the sediments, and the long stratigraphic ranges of the species.

## Materials and Methods

Kanaya and Koizumi (1966) analyzed the geographical distribution of diatom species in modern sediments using the uppermost layers of deep-sea cores collected from the Pacific Ocean ranging in latitude from 55°N to 55°S. We used 85 of the sediment samples from Kanaya and Koizumi (1966) (serial nos. 1–88 in Appendix 1). In addition, we used 61 core-top samples collected from the northwestern Pacific (Appendix 1 and Fig. 1a).

To correlate the distributions of *Thalassionema* species and the morphological types of the variants of *Thalassionema* species in the sediments with modern gyral circulations and current systems over the sediments in the Pacific, four morphological characteristics (valve outline, length, width, and marginal areolae density) were measured under light microscopy (LM), and seven characteristics (areolar occlusions, marginal foramina shape, rimoportula placement, rimoportula habit and orientation relative to valvar plane, external opening of rimoportula, presence or absence of a small pore at each apex and an apical spine) were compared among the species and types using scanning electron microscopy (SEM) observations.

Prior to the distribution analyses of *Thalassionema* species and types in the modern sediments, we ranked the state of diatom valve preservation, particularly the degree of valve silica dissolution and fragmentation of valves, on a scale from 1 to 5. Samples that exhibited well- to

Table 1. *Thalassionema* species and their varieties.

Taxa	Basionym	literature
<i>Thalassionema bacillare</i> (Heiden) Kolbe	<i>Spinigera bacillaris</i> Heiden in Heiden & Kolbe 1928, p. 564, pl. 6, fig. 121	Kolbe 1955, p. 178; Simonsen 1992, p. 25, pl. 22, figs. 1–6
<i>Thalassionema capitulata</i> (Castracane) Hustadt	<i>Synedra capitulata</i> Castracane 1886, p. 52, pl. 25, fig. 13	Hustadt 1958, p. 139
<i>Thalassionema claviformis*</i> Schrader		Schrader 1973, p. 712, pl. 23, figs. 11, 15
<i>Thalassionema frauendorfii</i> (Grunow) Hallegraaff	<i>Thalassiothrix frauendorfii</i> (Grunow) Grunow in Cleve & Grunow 1880, p. 109	Hallegraaff 1986, p. 62
<i>Thalassionema hiroakiensis*</i> (Kanaya) Schrader	<i>Fragilaria hiroakiensis</i> Kanaya 1959, p. 104, pl. 9, figs. 11–15	Schrader 1973, p. 711
<i>Thalassionema nitzschoides</i> (Grunow)	<i>Synedra nitzschoides</i> Grunow 1862, p. 403	Mereschkowsky 1902, p. 78, figs. 1–27
<i>T. nitzschoides</i> var. <i>acuminatum</i> * (Grunow)	<i>Synedra nitzschoides</i> var. <i>acuminata</i> Grunow in Pantocsek 1886, p. 36, pl. 26, fig. 246	Peragallo, M. 1903, p. 923
<i>T. nitzschoides</i> var. <i>australe</i> Cleve-Euler		Cleve-Euler 1949, p. 11, fig. 12
<i>T. nitzschoides</i> var. <i>gracile</i> Heiden		Heiden & Kolbe 1928, p. 564, pl. 5, fig. 115; Simonsen 1992, p. 24, pl. 21, figs. 1–4
<i>T. nitzschoides</i> var. <i>incurvatum</i> Heiden		Heiden & Kolbe 1928, p. 564, pl. 5, fig. 117; Simonsen 1992, p. 24, pl. 21, figs. 13–15
<i>T. nitzschoides</i> var. <i>infundibulum</i> Heiden		Heiden & Kolbe 1928, p. 564, pl. 5, fig. 116; Simonsen 1992, p. 24, pl. 21, figs. 5–9
<i>T. nitzschoides</i> var. <i>lanceolatum</i> Grunow:		van Heurck 1881, pl. 43, figs. 8, 9
synonym- <i>Spinigera lanceolata</i> Heiden in Heiden & Kolbe 1928, p. 565, pl. 5, fig. 120; Simonsen 1992, p. 25, pl. 21, figs. 16–17		Heiden & Kolbe 1928, p. 564, pl. 5, fig. 118; Simonsen 1992, p. 24, pl. 21, figs. 10–12
<i>T. nitzschoides</i> var. <i>parvum</i> Heiden		

Table 1. (Continued).

Taxa	Basionym	literature
<i>Thalassioëma obtusum</i> * (Grunow) Andrews	<i>Thalassiothrix? nitzschioïdes</i> var. <i>obtusa</i> Grunow in van Heurck 1881, pl. 43, fig. 6	Andrews 1976, p. 21, pl. 7, figs. 6–8
<i>Thallasionema pseudonitzschioïdes</i> (Schuelle & Schrader) Hasle	<i>Thalassiothrix pseudonitzschioïdes</i> Schuette & Schrader 1982, p. 214, pl. 1, figs. 1–9, pl. 2, figs. 10–14, pl. 3, figs. 15–20, pl. 4, figs. 21–25, pl. 5, figs. 26–30	Hasle & Syvertsen 1996, p. 341
<i>Thallasionema robusta</i> * Schrader		Schrader 1973, p. 712, pl. 23, figs. 24, 35–37
<i>Thallasionema schraderi</i> * Akiba		Akiba 1982, p. 50, figs. 6–11
<i>Thallasionema synediforme</i> (Greville) Hasle: synonym- <i>Thallasionema javanicum</i> (Grunow) Hasle in Hasle and Syvertsen 1996, p. 341, pl. 56, fig. 1, pl. 57	<i>Asterionella synediformis</i> Greville, 1865, p. 4, pl. 5, figs. 5, 6	Hasle 1999, p. 54
<i>Spinigera capitata</i> Heiden		Heiden & Kolbe 1928, p. 564, pl. 5, fig. 119; Simonsen 1992, p. 24, pl. 22, figs. 7–10

\* extinct *Thallasionema* species and varieties

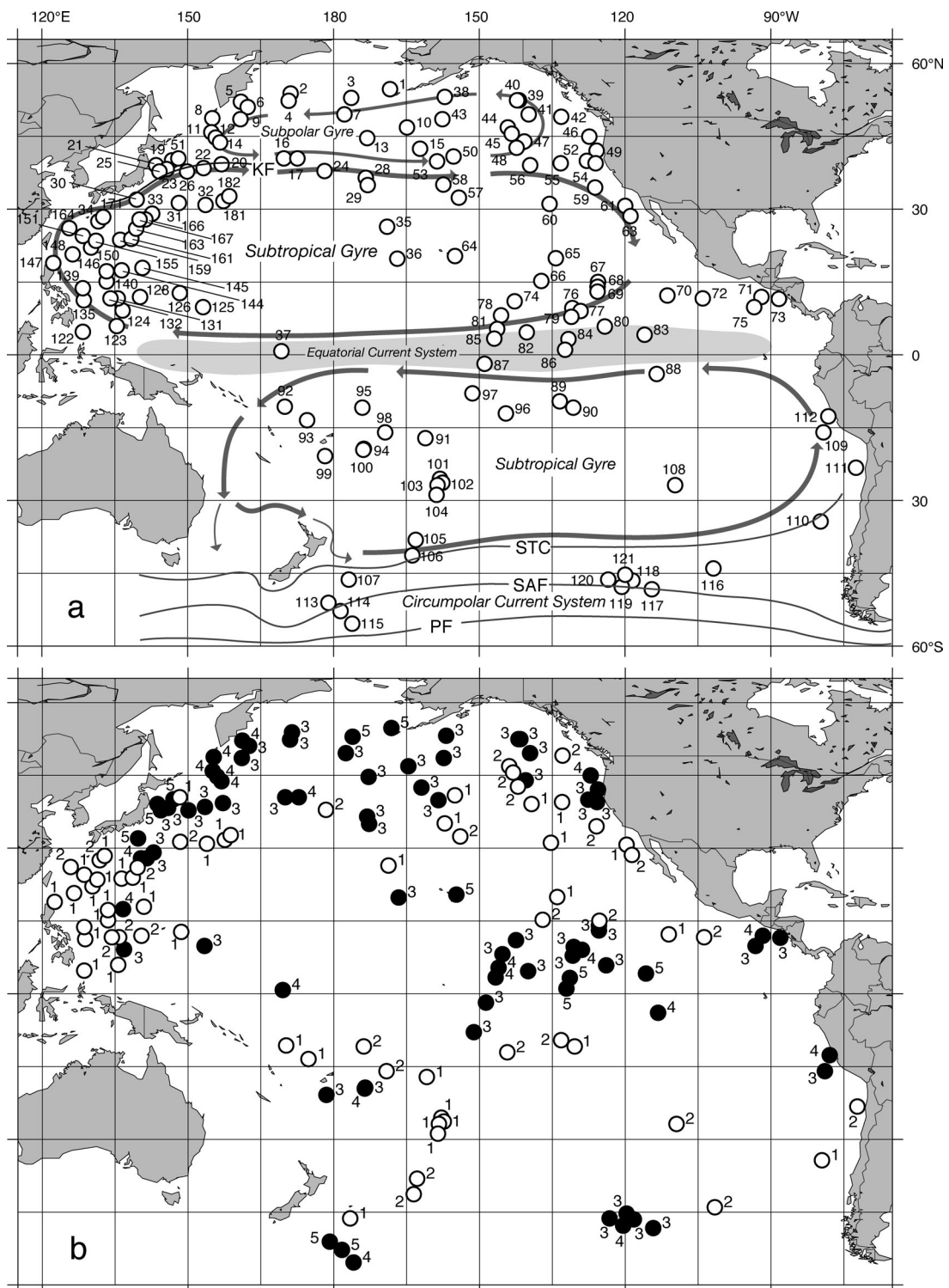


Fig. 1. Major gyral circulations and current systems in the Pacific Ocean and locations of 146 sediment cores (a). Serial numbers for the locations correspond to those in Appendix 1. State of valve preservation categorized into five classes (b). Top-cores with well- to moderately preserved valves ( $n=68$ ; classes 3–5) are indicated by solid circles. Gyral circulations and current systems in the Pacific are from Schmitz (1996) in Norris (2000) and Pahnke and Zahn (2005).

moderately-preserved valves (classes 3, 4, or 5) were used for analyses.

Observations and enumerations of both *Thalassionema* species and morphological types of the species were conducted at 1008x using a Zeiss Axioplan microscope equipped with Nomarskii differential interference contrast. The counting method followed Schrader and Gersonde (1978, fig. 1, E). Each slide was mounted with Pleurax or Styrax, and at least 100 half-valves (50 valves), and up to 700 half-valves (350 valves), were counted along transects under LM.

## Results

Diatom valves were generally well preserved in sediments under the Subpolar Gyre, the Equatorial Current System, and south of the Subtropical Convergence in the South Pacific. However, diatoms were poorly preserved in sediments under the central portions of the Subtropical Gyres in the North and South Pacific. Well- to moderately preserved valves occurred in 68 sediment samples (Appendix 2 and Fig. 1b).

We identified five *Thalassionema* species in the 68 samples: *T. bacillare* (Heiden) Kolbe, *T. frauenfeldii* (Grunow) Hallegraeff, *T. nitzschiooides* (Grunow) Mereschkowsky, *T. pseudonitzschiooides* (Schuette et Schrader) Hasle, and *T. synedriforme* (Greville) Hasle. We distinguished two morphological types of *T. bacillare* (*Ba* and *Bb*) and nine types of *T. nitzschiooides* (*Na*, *Nc*, *Nd-j*, incl. *T. nitzschiooides* s. s., *T. nitzschiooides* var. *incurvatum*, *T. nitzschiooides* var. *inflatum*, and *T. nitzschiooides* var. *parvum*; Table 2).

Types *Ba* and *Bb* of *T. bacillare* differed primarily in the position of the rimoportulae on the valves. Valves of type *Ba* exhibited a rimoportula close to an apex, whereas those of type *Bb* were on the valve face near an apex (Figs 58–64). Tanimura (1999) distinguished three morphological types in a variation of *T. nitzschiooides* s. l. Types *Na* (type *a* in the literature) and *Nc* (type *c* in the literature) were found in the Pacific sediments, and type *Nb* was identified as *T. pseudonitzschiooides*. Type *Nd* was also distinguished as a

probable morphological type of a morphological variant of *T. nitzschiooides* s. l. The isopole/slender valves of type *Nd* differed from those of types *Na* and *Nc*. Types *Ne* and *Nf* belong to the *T. nitzschiooides* vars. *incurvatum*, *inflatum* and *parvum* complex. Type *Nf* was more heavily silicified and had a coarser areolation of the valves than type *Ne*. Valve outlines allowed for the distinction among morphological types *Ng*, *Nh*, *Ni*, and *Nj*. Smaller valves of types *Ng* and *Nh* were similar in valve outline, but are distantly geographically distributed.

Based on their distribution, four groups of *Thalassionema* species and their morphological types were identified. The species and types in group 1 (*T. nitzschiooides* s. s. [*Na* and *Nc*], *T. nitzschiooides* s. l.? [*Nd*], and *T. pseudonitzschiooides*) were abundant in the sediments from the high-latitude North Pacific ranging from 40° to 60°N and common in the sediments under the coastal waters of the northwestern Pacific (Figs. 2a, 3). *Thalassionema frauenfeldii* was also common in the sediments from the northwestern Pacific, but not in the high-latitude northeastern Pacific (Fig. 4). The species and types of group 2 (two morphological types of *T. bacillare* [*Ba* and *Bb*] and *T. nitzschiooides* var. *incurvatum*, *T. nitzschiooides* var. *inflatum*, and *T. nitzschiooides* var. *parvum* [thinly to moderately silicified valve type: *Ne*]) ranged from common to abundant in the northern, equatorial, and southern Pacific, but not in the high latitudes of the ocean (Figs. 2b, 5). Three morphological types of *T. nitzschiooides* s. l. in group 3 (*Nh*, *Ni*, and *Nj*) were abundant in the sediments from the high-latitude South Pacific ranging in latitude from 45° to 60°S (Figs. 6c–e). The morphological types of group 4 (*T. nitzschiooides* var. ? [*Ng*] and *T. nitzschiooides* var. *incurvatum*, *T. nitzschiooides* var. *inflatum*, and *T. nitzschiooides* var. *parvum* [heavily silicified valve type: *Nf*]) ranged from common to abundant in the sediments from the eastern Pacific (Figs. 6a–b). *Thalassionema synedriforme* was rare in the sediments from the western Pacific (Fig. 6f).

Table 2a. *Thalassionema* species and their morphological types.

Taxa	<i>Thalassionema bacillare</i>		<i>T. frauenfeldii</i> <i>Bb</i>	Morphotype <b>a</b> in Tanimura (1999) <i>Na</i>	Morphotype <b>c</b> in Tanimura (1999) <i>Nc</i>	<i>T. nitzschioides</i> s. l. ? <i>Nd</i>
	<i>Ba</i>	<i>Bb</i>				
<b>Valve outline</b>	linear, with slightly inflated middle part of the valve and rounded apices* 97–230* 3–4*	linear, with slightly inflated middle part of the valve and rounded apices 105–? 2–5	linear, one apex tapering and the other apex rounded 65–164* 2–3*	linear, with rounded apices 7–25** 2.6–4**	linear lanceolate, with rounded apices 11–12**	linear, slender, with slightly inflated middle part of the valve and narrow-rounded apices 27–133 2.5–3.5
<b>Length (μm)</b>	7–12*	5–6	I-shaped bars, without fine side-branches small pores	Y-shaped bars, without fine side-branches small pores	Y-shaped bars, usually with fine side-branches small pores	Y-shaped bars, without fine side-branches small pores
<b>Width (μm)</b>	Y-shaped bars, with fine side-branches small pores	Y-shaped bars, with fine side-branches small pores	valve face-mantle junction sessile, diagonal to tangential	valve face-mantle junction sessile, nearly parallel to diagonal	valve face-mantle junction sessile, diagonal to tangential	valve face-mantle junction sessile, diagonal to tangential
<b>Marginal areola density (in 10 μm)</b>	7–12*	5–6	valve face tangential	valve face-mantle junction sessile, tangential	valve face-mantle junction sessile, nearly parallel to diagonal	valve face-mantle junction sessile, diagonal to tangential
<b>Areolar occlusions</b>	Y-shaped bars, with fine side-branches small pores	Y-shaped bars, with fine side-branches small pores	sessile, nearly parallel	sessile, tangential	sessile, nearly parallel to diagonal	sessile, diagonal to tangential
<b>Foramina</b>	valve face-mantle junction sessile, diagonal to tangential	valve face tangential	a short tube—a simple pore absent	a short tube—a simple pore present	a short tube present	a short tube—a simple pore present
<b>Rimoporella placement</b>	valve face-mantle junction sessile, diagonal to tangential	valve face tangential	a short tube—a simple pore absent	a short tube present	a short tube present	a short tube present
<b>Habit and slit orientation relative to the valvar plane</b>	valve face-mantle junction sessile, diagonal to tangential	valve face tangential	a short tube—a simple pore absent	a short tube present	a short tube present	a short tube present
<b>External opening</b>	a short tube—a simple pore absent	a short tube—a simple pore absent	a short tube—a simple pore absent	a short tube present	a short tube present	a short tube present
<b>A small pore at each apex</b>	present, two	absent	present	absent	absent	absent
<b>Apical spine(s) Figures</b>	Hasle 2001, figs. 85–100	Figs. 20–25, 58–64	Figs. 15, 65–67	Figs. 7–8	Figs. 9–13, 68–71	Figs. 9–13, 68–71
<b>Distribution</b>	the northern and equatorial Pacific, but not high-latitude of the ocean	the northern, equatorial and southern Pacific, but not high-latitude of the ocean	mostly the northwestern Pacific	mainly the high-latitude North Pacific ranging in latitude from 40°N to 60°N	mainly the high-latitude North Pacific ranging in latitude from 40°N to 60°N	mainly the high-latitude North Pacific ranging in latitude from 40°N to 60°N
<b>Remarks</b>	Simonsen 1992, p. 25, pl. 22, figs. 1–6	Hasle 2001, p. 62, figs. 54–67	Tanimura 1999, plate I, figs. 1 & 2	Tanimura 1999, figs. 3 & 4		

\* Hasle (2001); \*\* Tanimura (1999)

Table 2b.

Taxa Morphologic characteristics/ morphological types	<i>Thalassionema nitzschioides</i>				
	var. <i>incurvatum</i>	var. <i>inflatum</i>	var. <i>parvum</i>	var. <i>incurvatum</i> (heavily silicified type)	var. <i>inflatum</i> (heavily silicified type)
		<i>Ne</i>			<i>Nf</i>
<b>Valve outline</b>	wider, linear, with concave sides and rounded apices	wider, linear, expanded in the middle, with rounded apices	wider, linear, with parallel—nearly parallel sides and rounded apices	wider, linear, with concave sides and rounded apices	wider, linear, with parallel—nearly parallel sides and rounded apices
<b>Length (μm)</b>	7–18**	12–73**	8–23**	10–20	25–130
<b>Width (μm)</b>	3.2–4**	3.8–6**	3.8–4.7**	3.5–4.5	6–7
<b>Marginal areolae density (in 10 /μm)</b>	10–11	10–12	10–12	7–9	7–9
<b>areolar occlusions</b>	Y-shaped bars, with well-developed side-branches	Y-shaped bars, with well-developed side-branches	Y-shaped bars, with well-developed side-branches	Y-shaped bars, with well-developed side-branches	Y-shaped bars, with well-developed side-branches
<b>foramina</b>	small pores	small pores	small pores	small pores	small pores
<b>Rimoporella placement</b>	valve face-mantle junction	valve face-mantle junction	valve face-mantle junction	valve face-mantle junction	valve face-mantle junction
<b>habit and orientation relative to the valvar plane</b>	sessile, diagonal	sessile, diagonal	sessile, nearly parallel to diagonal	sessile, diagonal	sessile, nearly parallel to diagonal
<b>external opening</b>	a short tube—a simple pore	a short tube—a simple pore	a short tube—a simple pore	a short tube—a simple pore	a short tube—a simple pore
<b>A small pore at each apex</b>	present	present	present	present	present
<b>Apical spine(s)</b>	absent	absent	absent	absent	absent
<b>Figures</b>	Figs. 28–33			Figs. 34–40	
<b>Distribution</b>	the northern, equatorial and southern Pacific, but not high-latitude of the ocean				
<b>Remarks</b>	Tanimura 1999, pl. III, fig. 4	Tanimura 1999, pl. III, figs. 5 & 6	Tanimura 1999, pl. III, figs. 1–3	incl. <i>Spinigera capitata</i>	

\*\* Tanimura (1999)

Table 2c.

Mor-phologic characteristics/ morphological types	<i>Thalassionema nitzschilioides</i> s. l.				<i>T. pseudomitschilioides</i>	<i>T. syndriforme</i>	<i>T. pseudomitschilioides</i>
	<i>Ng</i>	<i>Nh</i> (=Ng?)***	<i>T. nitzschiooides</i> var. <i>lanceolata</i> ? <i>Ni</i>	<i>Nj</i>			
<b>Valve outline</b>	wider, linear, expanded in the middle, with slightly capitated apices	wider, linear, expanded in the middle, with slightly capitated apices	wider, linear, expanded in the middle, with narrow-capitated apices	linear, with capitated apices	spatulate, narrow close to the wide rounded end and tapering towards the other	linear, tapering towards one end*	
<b>Length (μm)</b>	55–145	35–90	60–130	120–170	135–350 ***	10–200***	
<b>Width (μm)</b>	6–7	6–6.5	6.5–7.5	4–4.5	2–6 *	2–4 *	
<b>Marginal areolae density (in 10 μm)</b>	7–10	9–11	10–11	9–11	12–16 *	9–11 *	
<b>areolar occlusions</b>	Y-shaped bars, with fine side-branches	Y-shaped bars, with fine side-branches	Y-shaped bars, with fine side-branches	Y-shaped bars	elaborate bars? (Hasle 2001, figs. 76–78)	Y-shaped bars, without fine side-branches	
<b>foramina</b>	small pores	small pores	small pores	small pores	small pores	small pores	
<b>Rimoporella placement</b>	valve face-mantle junction	valve face-mantle junction	valve face-mantle junction	valve face-mantle junction	valve face-mantle junction	valve face-mantle junction	
<b>habit and orientation relative to the valvar plane</b>	sessile, diagonal	sessile, diagonal	sessile, diagonal	sessile, diagonal	sessile, diagonal to tangential	sessile, diagonal	
<b>external opening</b>	a simple pore	a simple pore	a simple pore	a simple pore	a large, long depression	a short tube	
<b>A small pore at each apex</b>	present	present	absent	absent	present	present	
<b>Apical spine(s) Figures</b>	absent Figs. 50–55	absent Figs. 17–18, 19 ?	Figs. 41–44	Figs. 46–47	Fig. 16	Figs. 14, 72–74	
<b>Distribution</b>	the western Pacific	the high-latitude South Pacific ranging in latitude from 45°S to 60°S	the high-latitude South Pacific ranging in latitude from 45°S to 60°S	the high-latitude South Pacific ranging in latitude from 45°S to 60°S	the western Pacific	mainly the high-latitude North Pacific	
<b>Remarks</b>	*** Ng and Nh were similar in valve outline, but are distantly geographically distributed.				Hasle 2001, figs. 68–84	Hasle 2001, figs. 28–42	

\* Hasle (2001); \*\*\* Shuette and Schrader (1982); \*\*\*\* Hustedt in Meister (1932)

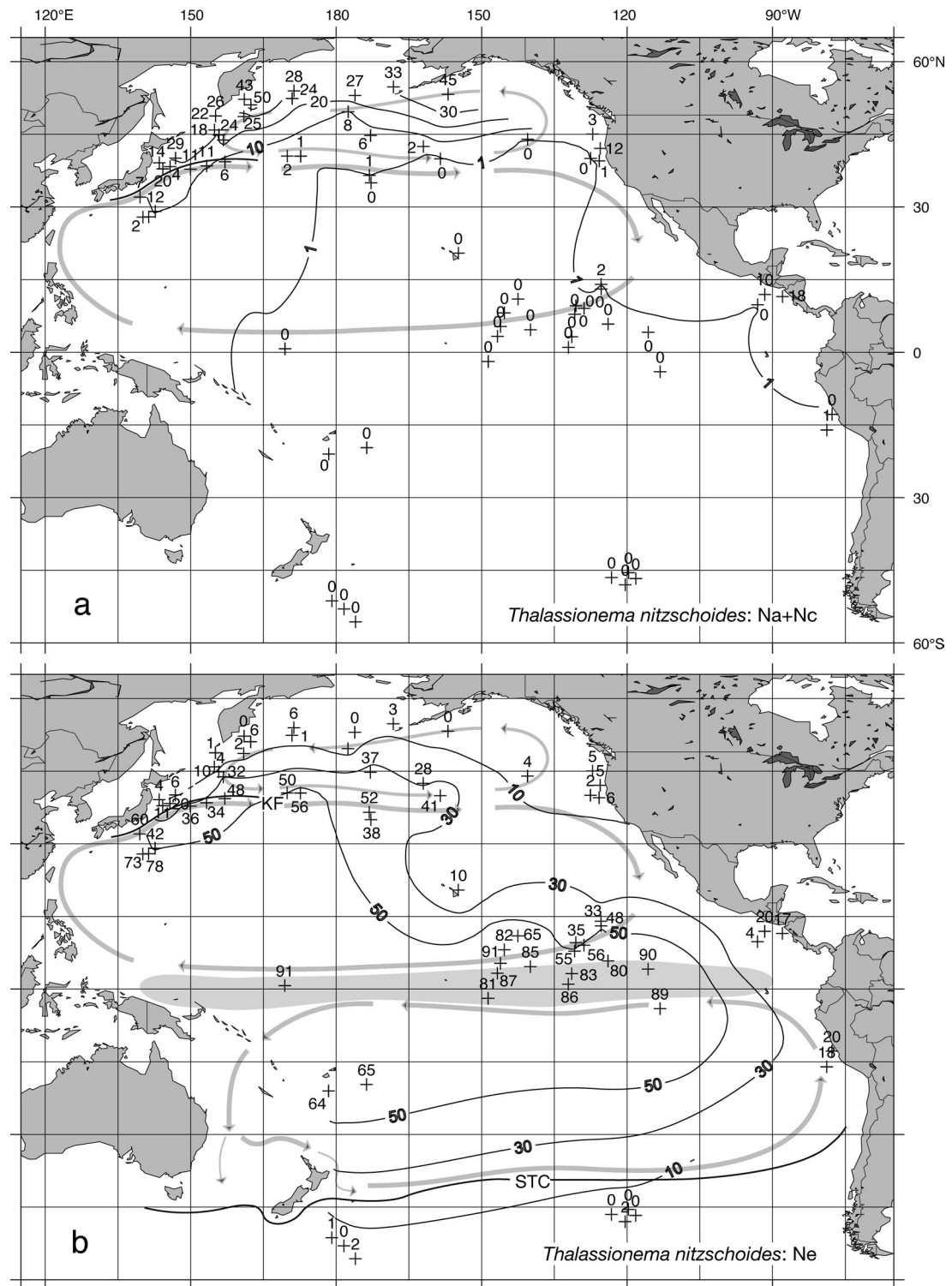


Fig. 2. Contour maps of percent abundances for three morphological types of a morphological variant of *T. nitzschoides* s. l. (**a**: *Na+Nc*; **b**: *Ne*) out of the total *Thalassionema* spp. counts.

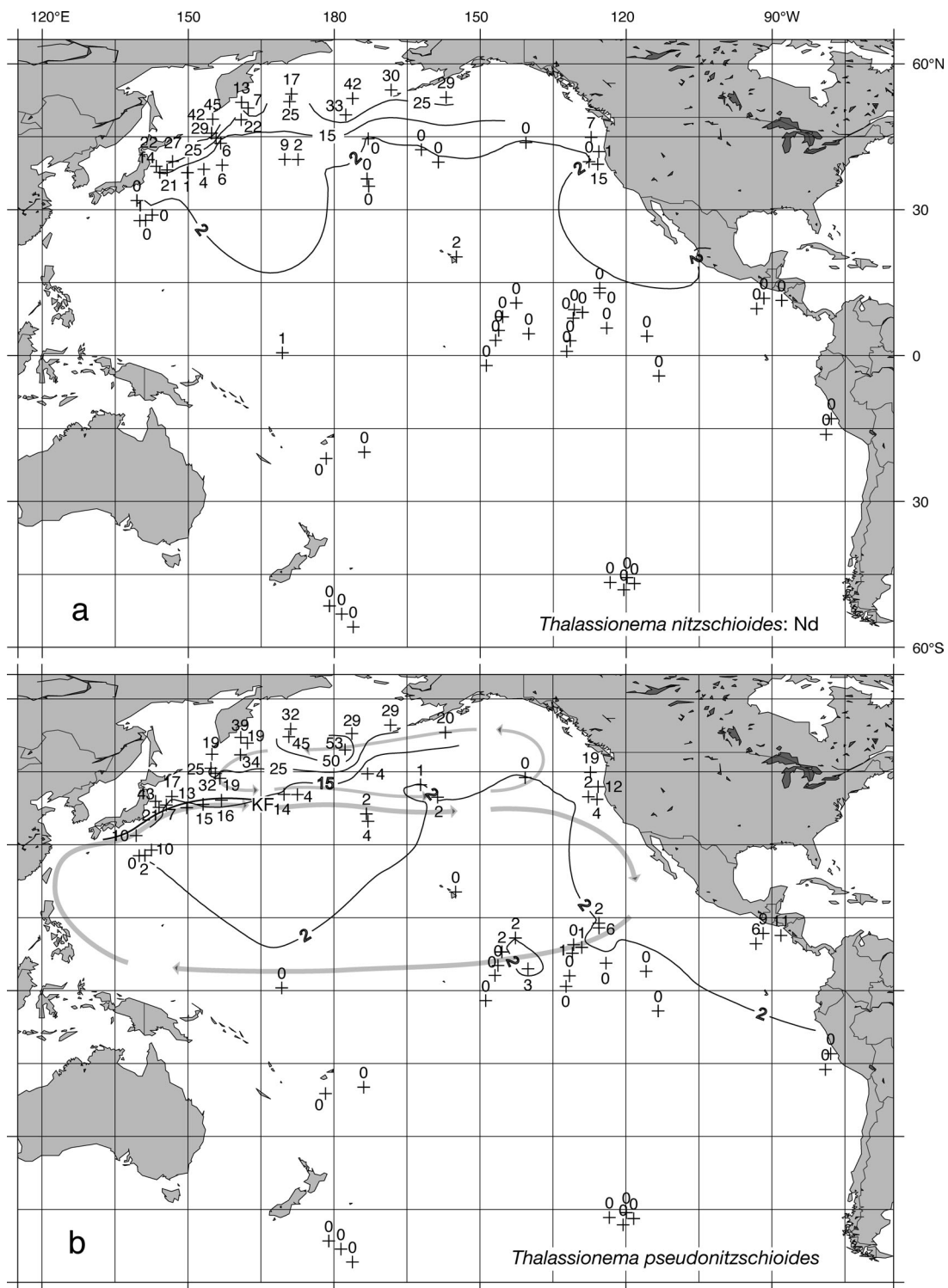


Fig. 3. Contour maps of percent abundances for one morphological type of a morphological variant of *T. nitzschoides* s. l. (a: *Nd*) and for *T. pseudonitzschoides* (b) out of the total *Thalassionema* spp. counts.

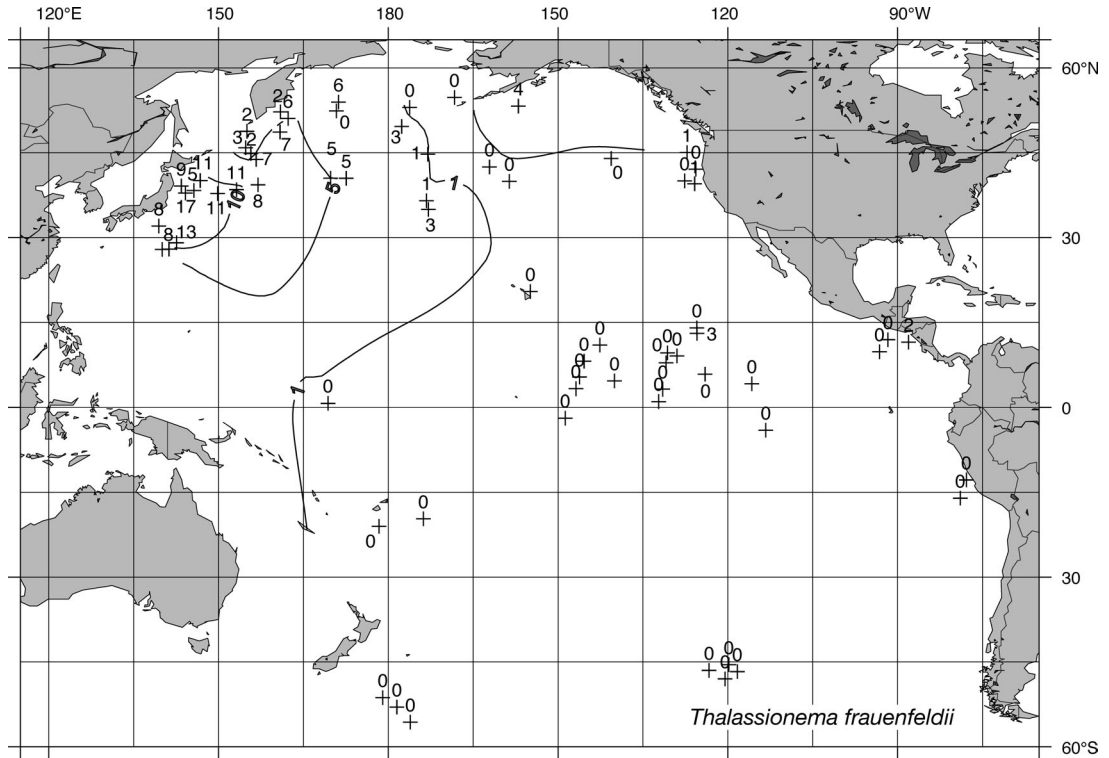


Fig. 4. Contour map of percent abundances for *T. frauenfeldii* out of the total *Thalassionema* spp. counts.

## Discussion

Surface water circulation systems in the Pacific consist of three gyral circulations and two current systems, specifically (from north to south) the Subpolar Gyre, the Subtropical Gyre in the North Pacific, the Equatorial Current System, the Subtropical Gyre in the South Pacific, and the Circumpolar Current System (Schmitz, 1996; Norris, 2000, fig. 3; Fig. 1). Some oceanic fronts are formed among gyres and/or current systems. For example, the Kuroshio Front (KF in Fig. 1) is formed between the Subpolar Gyre (the Oyashio Current) and the Subtropical Gyre (the Kuroshio Current) in the northwestern Pacific (Kawai, 1972), and the Subtropical Convergence (STC in Fig. 1) is formed between the Subtropical Gyre and the Circumpolar Current System in the South Pacific (Pahnke and Zahn, 2005).

We found strong correlations between the distributions of *T. pseudonitzschoides*, *Ba*, *Bb*, *Na*,

*Nc*, *Ne*, and *Nd* in the sediments and the gyral circulations and current systems over the sediments. However, we did not observe any correlations between the distributions of *Ng*, *Nf*, and *T. frauenfeldii* and any specific gyral circulation and/or current system in the Pacific. Group 1 (*T. nitzschoides* s. s. [*Na* and *Nc*], *T. nitzschoides* s. l.? [*Nd*], and *T. pseudonitzschoides*) were primarily distributed in the sediments under the Subpolar Gyre, off of the North American continent and northwest of the Kuroshio Front. The southern to southwestern reaches of the distributions of species and morphological types corresponded well with the Kuroshio Front.

In contrast to group 1, the morphological types in group 3 (*Nh*, *Ni*, and *Nj*) were widely distributed in the sediments under the Circumpolar Current System. These results suggest that the three types are common in waters south of the Subtropical Convergence, which may indeed serve as the northern boundary of the distribution

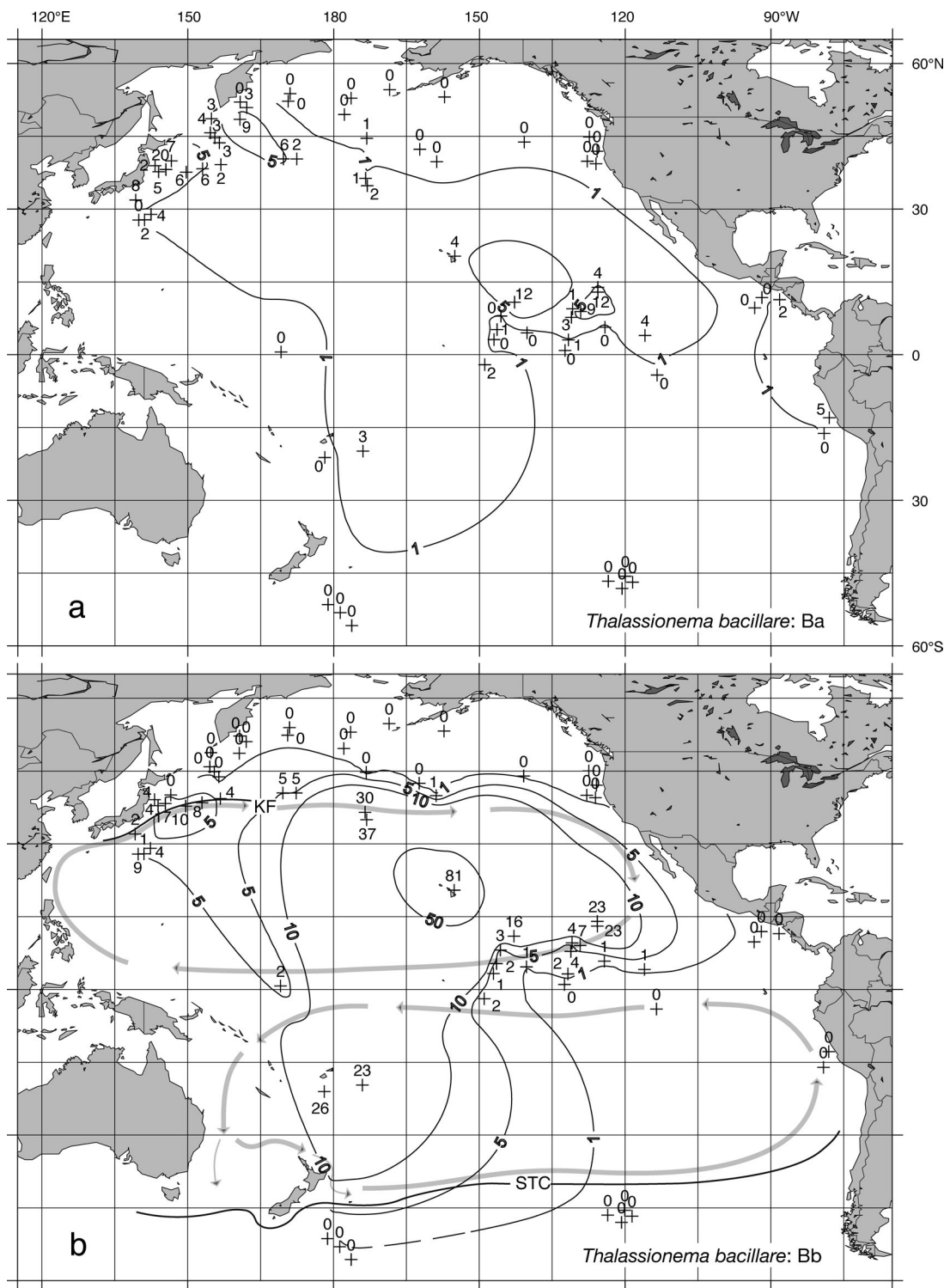


Fig. 5. Contour maps of percent abundances for two morphological types of a morphological variant of *T. bacillare* (a: Ba, b: Bb) out of the total *Thalassionema* spp. counts.

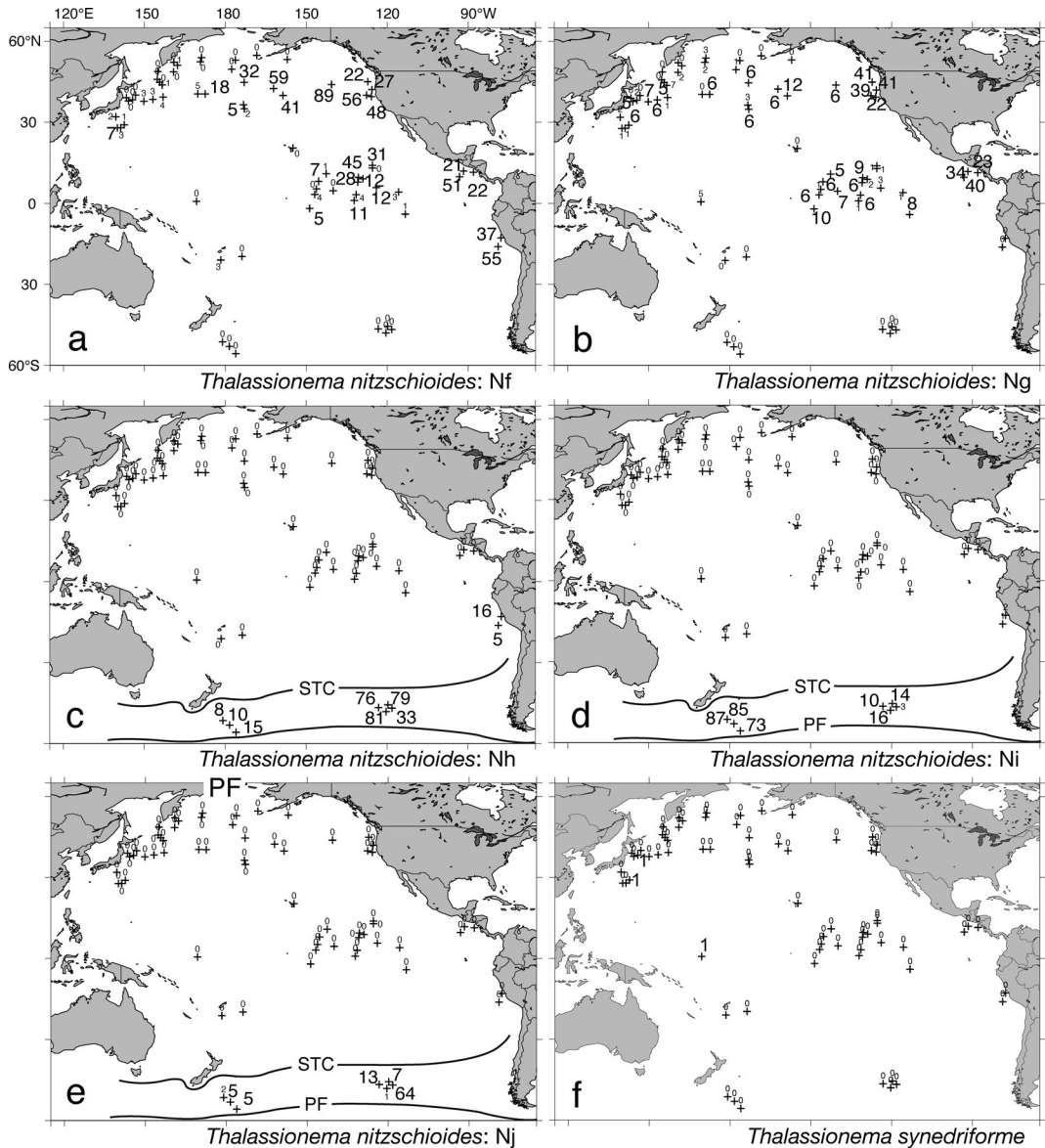


Fig. 6. Distributions of percent abundances for five morphological types of a morphological variant of *T. nitzschioides* s. l. (a–e: Nf–Nj) and for *T. synedriforme* (f) out of the total *Thalassionema* spp. counts.

of these morphological types. However, the distribution of *Thalassionema* species in the Subtropical Gyre of the South Pacific is not clear because of the poor preservation of diatom valves in the gyre.

The distribution of the *Thalassionema* types in group 2 (*Ba*, *Bb*, and *Ne*) occurred between the distributions of groups 1 and 3; that is, these

types were widely distributed in the sediments under the Subtropical Gyres in the North and South Pacific and under the Equatorial Current System. Types *Ba* and *Bb* were distributed in the sediments under the Subtropical Gyres of the North and South Pacific and were more abundant under the central to southeastern portion of the Subtropical Gyre in the North Pacific. The north-

ern to northeastern reaches of the distribution of types *Ba* and *Bb* corresponded well with the Kuroshio Front. Type *Ne* was primarily restricted to the sediments within the Subtropical Gyres of the North and South Pacific and in the Equatorial Current System and was particularly abundant in the sediments under the central to southeastern portion of the Subtropical Gyre in the North Pacific. The north-northeastern boundary of the distribution of type *Ne* also corresponded well with the Kuroshio Front.

The observed distributions of the *Thalassionema* species and morphological types strongly suggest that two oceanic fronts, the Kuroshio Front and the Subtropical Convergence, form the boundaries for the distributions of groups 1–3 in the Pacific. These modern fronts likely serve as barriers to the southward migration of the species and types of group 1 and to the northward migration of group 3.

The morphological types of group 4 (*Nf* and *Ng*) were primarily distributed in the northeastern region of the Pacific. However, we did not observe any correlations between the distribution of group 4 and a modern gyral circulation and/or current system in the Pacific. *Thalassionema frauenfeldii* was primarily restricted to sediments under the northwestern part of the ocean.

We observed strong correlations between the distributions of several *Thalassionema* species and morphological types in the sediments and the gyral circulations and current systems over the sediments in the Pacific. These results suggest that future studies of the distribution of *Thalassionema* species in the 15-Ma, 10-Ma, and 5-Ma horizons in the Pacific may elucidate the mechanisms of the diversification of *Thalassionema* species and of diatoms in general. The allopatric distribution of diatom assemblages driven by the evolution of surface water circulation systems in the Pacific may have affected the diversification of *Thalassionema* species. Indeed, allopatric speciation may explain the appearance of modern *Thalassionema* species and their morphological types through rapid speciation in isolated populations, followed by the differentiation of water

masses caused by changes in surface water circulation systems. Examples of such changes include the intensification of the Subtropical Gyre approximately 15 Ma (Kennett *et al.*, 1985) and the formation of the Subpolar Gyre at 2.5 Ma (Sancetta and Silvestri, 1986).

In addition, future studies should determine whether the observed morphological types of *Thalassionema* species constitute new taxa. Such studies should focus on the historical changes in the distributions of these morphological types in the Pacific, as well as their differentiation within morphological variants of a single *Thalassionema* species. For example, the distributions of the morphological types within a variant of *T. bacillare* were similar, whereas the distributions of the types of *T. nitzschiooides* differed. Therefore, *T. nitzschiooides* var. *incurvatum*, *T. nitzschiooides* var. *inflatum*, and *T. nitzschiooides* var. *parvum* may represent a new single taxon.

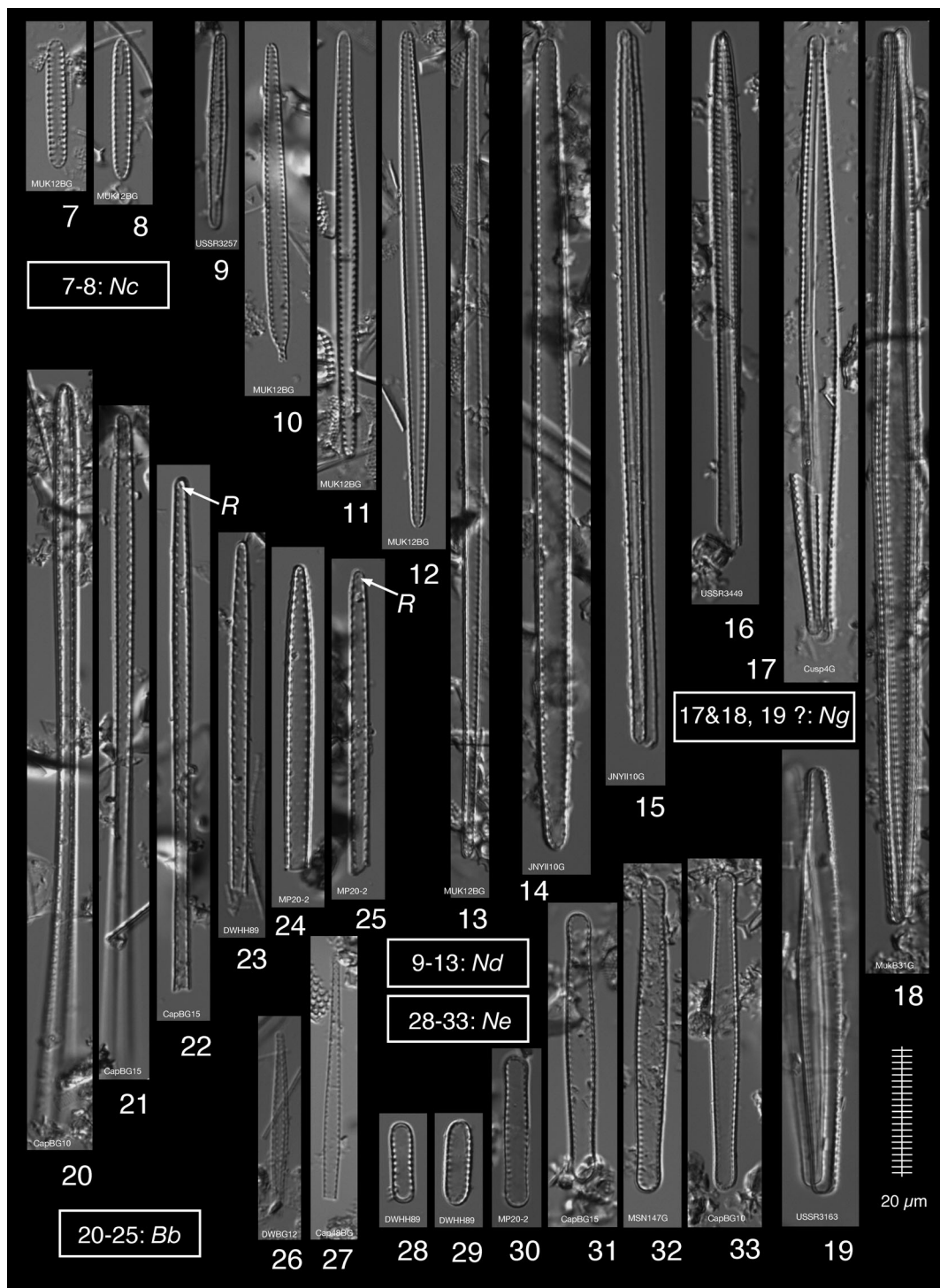
#### Taxonomic Notes

*Thalassionema bacillare* (Heiden) Kolbe 1955,  
p. 178

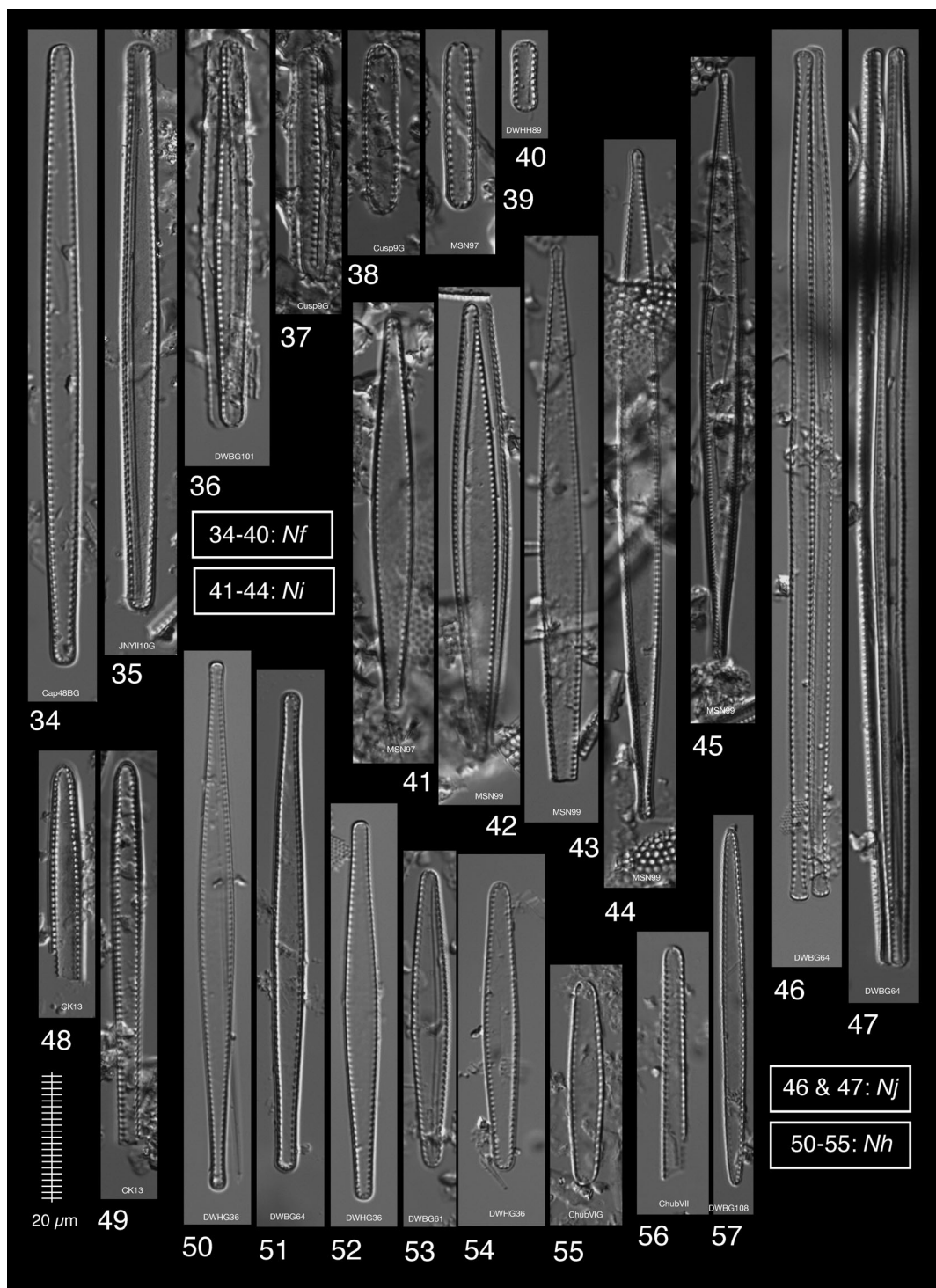
Two different morphological types of *T. bacillare* were found in the Pacific sediments (Table 2), one of which (type *Bb*; Figs. 20–25; 58–64) is that discerned in Simonsen (1992) from the types of Hiden and Kolbe (1928). The second type (*Ba*) is the form observed, described, and illustrated by Hasle (2001, p. 29–32, figs 85–100). Valves of type *Bb* have a rimoportula on the valve face near an apex, whereas the valves of type *Ba* have a rimoportula close to an apex. The valve face rimoportulae are visible under LM and are depicted in the figures of Simonsen (1992, plate 22, figs. 1, 6).

*Thalassionema nitzschiooides* var. *incurvatum*, *T. nitzschiooides* var. *inflatum*, and *T. nitzschiooides* var. *parvum*

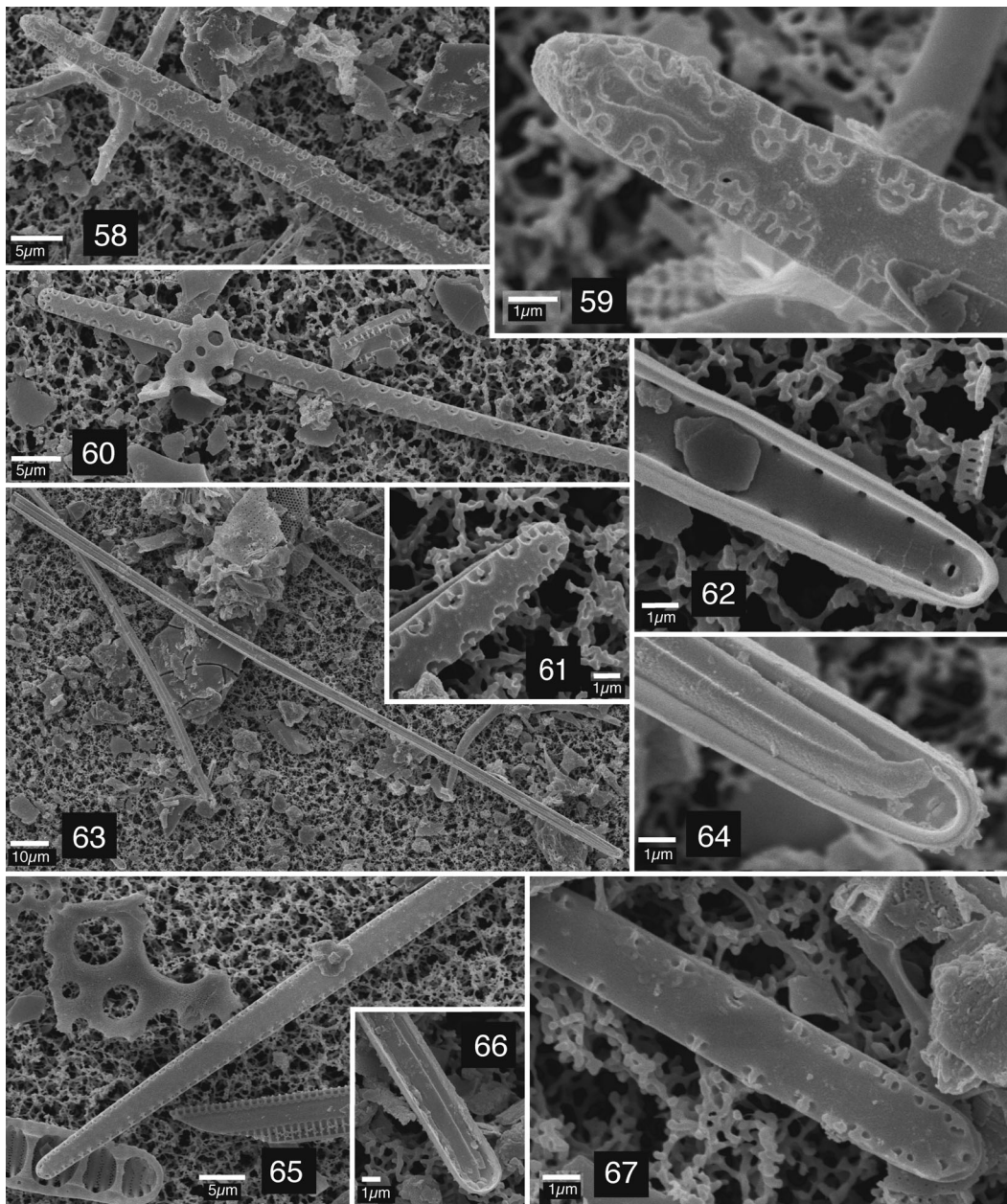
Except for differences in valve outline, these three taxa exhibit the same morphological characteristics (Table 2), and transitory forms among them are commonly found in the present study.



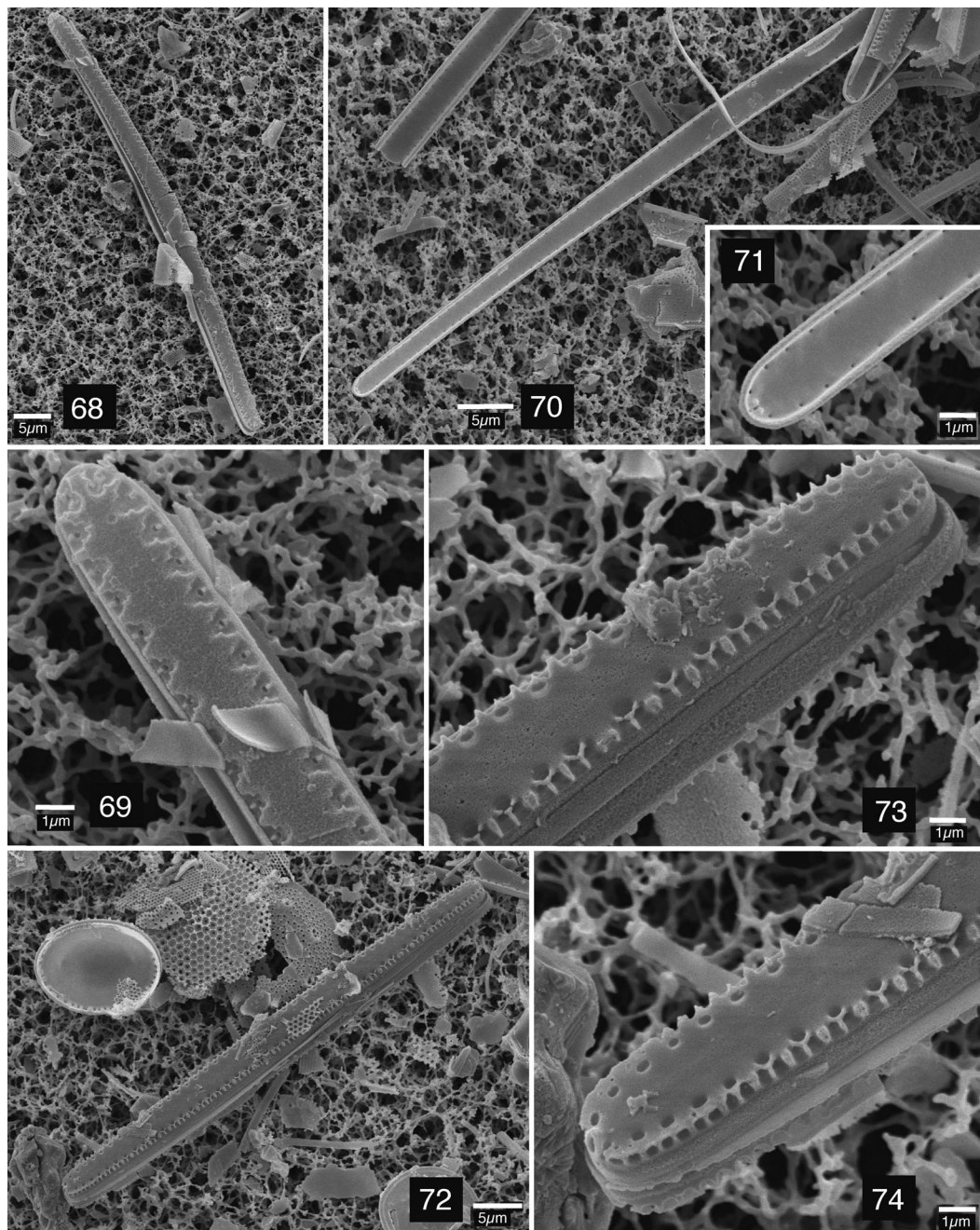
Figs. 7–33. Light microscopy micrographs of one morphological type of *T. bacillare* (*Bb*), *T. frauenfeldii*, four types of *T. nitzschioiodes* (*Nc*, *Nd*, *Ne* and *Ng*), *T. pseudonitzschioiodes*, *T. synedriforme* and *Thalassionema* ? sp. 7 & 8, *Nc*; 9–13, *Nd*; 14, *T. pseudonitzschioiodes*; 15, *T. frauenfeldii*; 16, *T. synedriforme*; 17 & 18, *Ng*; 19, *Ng* ?; 20–25, *Bb*; 26 & 27, *Thalassionema* ? sp.; 28–33, *Ne*. Sample names at the bottom of each figure correspond with those in Appendix 1. Each arrow labeled with the letter *R* in Figs. 22 and 25 indicates a rimoprotula.



Figs. 34–57. Light microscopy micrographs of four morphological types of *T. nitzschiooides* (*Nf*, *Nh*, *Ni* and *Nj*) and *Thalassionema* ? spp. 34–40, *Nf*; 41–44, *Ni*; 45, *Thalassionema nitzschiooides* var.; 46 & 47, *Nj*; 48 & 49, *Thalassionema* ? sp.; 50–55, *Nh*; 56, *Thalassionema* ? sp.; 57, *Thalassionema* sp. Sample names at the bottom of each figure correspond with those in Appendix 1.



Figs. 58–67. Scanning electron microscopy micrographs of one morphological type of *T. bacillare* (Bb) and *T. frauenfeldii*. 58–64, Bb; 58 & 59, external view of a half-valve, detail showing an external opening of rimoportula near the apex and external openings of marginal areolae with Y-shaped bars having fine side branches (V21-83); 60, external view of a half-valve (MP20-2); 61, an external opening of rimoportula (MP20-2); 62, internal view of an apex, showing a rimoportula (V21-83). 63 & 64; internal view of a half-valve, detail showing a rimoportula (V21-83). 65–67, *T. frauenfeldii*; 65, external view of a half-valve (TP-71); 66, internal view of a half-valve, showing a rimoportula (JYNII-10G); 67 external view of a half-valve, showing external openings of marginal areolae with I-shaped bars (V21-83).



Figs. 68–74. Scanning electron microscopy micrographs of one morphological type of *T. nitzschiooides* (*Nd*) and *T. pseudonitzschiooides*. 68–71, *Nd*; 68 & 69, external view of a frustule, detail showing an external opening of rimoportula at the apex and external openings of marginal areolae (Muk12BG); 70 & 71, internal view of a half-valve, detail showing an rimoportula at the apex (Muk12BG). 72–74, *T. pseudonitzschiooides*, external view of a frustule, details showing the external openings of rimoportulae near the apices and external openings of marginal areolae with Y-shaped bars having no fine side branches (Muk12BG).

Kolbe (1954) placed *T. nitzschiooides* var. *incuvatum* and *T. nitzschiooides* var. *inflatum* into synonymy with *T. nitzschiooides* var. *parvum*. However, we observed two different types of the morphological continuity of these three varieties. Type *Nf* (Figs. 34–40) has denser areolations (7–9 in 10 µm) and thicker valves, similar to species reported from the Gulf of Mexico and Baja California (Moreno-Ruiz and Licea, 1995, figs. 15, 20–22). The other type has the morphological continuity described as typical for *T. nitzschiooides* var. *incurvatum*, *T. nitzschiooides* var. *inflatum*, and *T. nitzschiooides* var. *parvum* (Figs. 28–33), similar to forms reported from the northwest Pacific (Tanimura, 1999, plate III, figs. 1–6).

#### Other *Thalassionema* species, their varieties, and allied forms

Hustedt (1958, p. 139) placed *Spinigera capitata* Heiden (Heiden and Kolbe, 1928, p. 565, pl. 5, fig. 119) in synonymy with *T. capitulata* (Castracane) Hustedt (Basionym: *Synedra capitulata* Castracane, 1886, p. 52, pl. 25, fig. 13). However, *Spinigera capitata* (depicted in Heiden and Kolbe, 1928, pl. 5, fig. 119 and photographed from type slides by Simonsen, 1992, pl. 22, figs. 7?10) appears to differ from *Synedra capitulata* (Castracane, 1886, pl. 25, fig. 13; Hasle, 1960, fig. 3) in the shape of the apices, with the latter species displaying much more conspicuously capitated apices. In contrast, *Spinigera capitata* exhibits the same morphological characteristics as *T. nitzschiooides* var. *inflatum*. We included *Spinigera capitata* in *T. nitzschiooides* var. *inflatum* (the morphologic type *Nf*), and *T. capitulata* was not found in our samples. *Thalassionema nitzschiooides* var. *gracile* Heiden and Kolbe (1928, p. 564, pl. 5, fig. 115) rarely occurred in the core-top samples, and we bundled it into *Thalassionema* spp. *Thalassionema nitzschiooides* var. *lanceolata* Grunow in Van Heurck (1881, pl. 43, figs. 8, 9) was also rare in the samples, and we included it in the morphologic type *Ni*.

#### Acknowledgments

The sediment samples used in this study were collected in the 1990s by the Geological Survey of Japan, the Lamont-Doherty Earth Observatory, the Ocean Research Institute of the University of Tokyo, Ryukyu University, and the Scripps Institution of Oceanography. We thank Drs. Megumi Saito and Matthew L. Julius for many helpful suggestions, and Mr. Fumio Akiba for his constructive review. This study was financially supported by the research program “Historical development and origin of biodiversity under the global environmental dynamics” of the National Museum of Nature and Science, Tokyo, Japan.

#### Appendix 1. Sediment core-tops studied.

Ser. No.	Sample Name	Latitude	Longitude	Water Depth
1	MUK12BG	54.46 N	168.19 W	1960
2	TP40-1	53.57 N	171.11 E	1382
3	CK8	53.01 N	176.15 W	3660
4	USSR3357	52.23 N	170.48 E	6983
5	USSR3403	52.13 N	160.55 E	4435
6	USSR3274	51.04 N	162.17 E	5437
7	CK11	49.39 N	177.39 W	4850
8	USSR3257	48.47 N	155 E	6948
9	USSR3114	48.39 N	160.51 E	5571
10	CK6	46.57 N	164.49 W	5094
11	USSR3109	45.53 N	154.47 E	5001
12	USSR3108	44.51 N	155.42 E	4902
13	CK13-3	44.45 N	173.02 W	4835
14	USSR3163	43.49 N	156.38 E	5441
15	CK4	42.29 N	162.08 W	5388
16	JYNII-10G	40.3 N	169.48 E	5550
17	JYNII-8G	40.29 N	172.33 E	4250
19	TP71	40.05 N	146.45 E	5300
20	JYNII-14G	39.19 N	156.57 E	5050
21	Takuyo6	39.06 N	143.24 E	5635
22	JYNII-17G	38.28 N	153.1 E	5690
23	USSR3449	38.19 N	145.38 E	5690
24	JYNII-6G	37.56 N	178.1 E	3449
25	USSR3225	37.51 N	144.08 E	5250
26	JYNII-19	37.46 N	149.49 E	5090
28	CK16	36.3 N	173.16 W	5910
29	USSR4084	34.59 N	172.56 W	6547
30	TP97	32.02 N	139.25 E	4195
31	USSR3478	31.17 N	148.5 E	5971
32	USSR3206	30.57 N	153.33 E	1336
33	USSR3493	29.04 N	142.34 E	6177
34	USSR3530	27.31 N	131.32 E	5194
35	CK22	26.22 N	168.53 W	5194
36	MP24	19.45 N	166.5 W	4963
37	Cap2BG1	0.43 N	169.2 E	4450

Ser. No.	Sample Name	Latitude	Longitude	Water Depth	Ser. No.	Sample Name	Latitude	Longitude	Water Depth
38	MukB10G	53.15 N	157.02 W	5200	97	MSN131PG	8 S	151.2 W	—
39	MukB21G	52.32 N	141.44 W	4320	98	CapHG19	16.05 S	169.15 W	5340
40	MukH27G	52.31 N	142.06 W	4560	99	CapBG10-3	21.01 S	178.34 E	—
41	USSR4151	49.38 N	139.42 W	3792	100	CapBG15	19.42 S	173.49 W	3580
42	Univ.Wash.144-10	49.04 N	133 W	3970	101	MSN125G	25.4 S	158 W	—
43	NthHol8	48.37 N	157.29 W	3970	102	MSN124G	26.3 S	157.3 W	—
44	USSR4158	46.57 N	144 W	3357	103	MSN123G	27 S	158.3 W	—
45	Cusp11G	45.34 N	143.11 W	5715	104	MSN121G	29 S	158.4 W	—
46	Cas2	45.02 N	127.13 W	4658	105	MSN113G	38.2 S	163 W	—
47	Cusp9G	43.58 N	140.38 W	4700	106	MSN111G	41.3 S	163.4 W	—
48	MukH5G	42.41 N	142.09 W	2930	107	MSN109P	46.3 S	176.46 W	4637
49	MukB31G	42.05 N	125.39 W	4450	108	DWBG121	27 S	109.3 W	—
50	NthHol9	40.53 N	155.12 W	4290	109	DWBG101	16.03 S	78.56 W	4280
51	NthHol11	40.31 N	147.58 W	2917	110	DWHH58	34.3 S	79.3 W	3780
52	USSR4183	40.01 N	127.39 W	5343	111	DWBG87	23.24 S	72.1 W	4260
53	CK3	39.56 N	158.38 W	5370	112	DWBG108	12.49 S	77.51 W	2300
54	Csp4G	39.3 N	125.52 W	4460	113	MSN100G	51.2 S	179 E	—
55	Men18	39.3 N	133.05 W	5005	114	MSN99G	53 S	178.3 W	—
56	Men27	39.05 N	139.26 W	3733	115	MSN97G	55.39 S	176.08 W	5200
57	NthHol12	32.27 N	154.08 W	4740	116	DWBG77	44.09 S	101.34 W	3820
58	CK2	35.09 N	157.17 W	5920	117	DWBG68	48.27 S	114.18 W	—
59	Cusp24G	34.29 N	126.02 W	5582	118	DWBG64	46.43 S	118.2 W	—
60	Cusp2G	31.05 N	135.24 W	5627	119	DWBG63	48 S	120.3 W	—
61	FanBG7	30.43 N	119.5 W	4760	120	DWBG61	46.3 S	123.2 W	—
63	FanHMS5	28.35 N	118.42 W	5160	121	DWHG-36	45.3 S	119.5 W	—
64	MP20-2	20.27 N	154.55 W	3900	122	V20-148	4.44 N	128.3 E	5879
65	USSR4293	19.56 N	134.05 W	5664	123	V20-146	5.55 N	135.31 E	4702
66	MSN155G	15.09 N	137.06 W	3470	124	V20-145	9.08 N	136.52 E	4702
67	Chub3	15 N	125.26 W	5100	125	KH80-3-30	9.5 N	153.14 E	5480
68	Chub4	14.01 N	125.29 W	5277	126	KH80-3-27	12.42 N	148.3 E	5930
69	Chub5	13.03 N	125.28 W	4992	128	V19-110	11.52 N	140.1 E	3523
70	ChubXIIIG	12.13 N	111.03 W	4380	131	V19-112	11.38 N	135.5 E	5960
71	ChubVIG	11.56 N	91.43 W	4505	132	V19-113	11.34 N	134.01 E	5687
72	ChubXIG	11.38 N	103.48 W	4448	135	V19-117	11.12 N	128.46 E	5565
73	ChubVII	11.3 N	88.04 W	3331	139	V21-125	13.41 N	128.29 E	5433
74	MSN150G	10.59 N	142.37 W	3563	140	V21-122	15.07 N	133.2 E	4767
75	ChubVIIIG	9.48 N	93.12 W	3257	144	V21-118	17.23 N	136.31 E	5280
76	DWBG6	9.36 N	130.41 W	4869	145	V21-117	17.54 N	140.59 E	4685
77	DWHT8	9.03 N	129 W	4978	146	V20-142	17.11 N	133.16 E	5097
78	MSN147G	8.07 N	145.25 W	3641	147	V21-133	18.57 N	122.23 E	1928
79	DWBG8	7.51 N	130.55 W	5003	148	V21-134	20.43 N	126.23 E	5298
80	Cap48BG1	5.49 N	124.02 W	4650	150	V21-114	22.08 N	130 E	5618
81	MSN142G	5.2 N	146.13 W	5100	151	V21-111	24.3 N	128.31 E	5616
82	MP11-1	4.39 N	140.03 W	5069	155	V21-101	23.33 N	131.01 E	4990
83	DWBG149	4.08 N	115.46 W	4125	159	V21-97	23.41 N	136.05 E	4868
84	DWBG12	3.12 N	131.31 W	5089	161	V21-95	23.57 N	138.31 E	4698
85	MSN141G	3.17 N	146.51 W	4400	163	V21-138	26.02 N	139.29 E	4418
86	DWBG13	1.01 N	132.14 W	4160	164	RN93, P5-1	26.09 N	125.5 E	1464
87	MSN136G	1.54 S	148.45 W	4438	166	V21-84	27.57 N	141.22 E	4116
88	DWHH89	4.02 S	113.18 W	4577	167	V21-83	27.54 N	140.03 E	3702
89	DWHH13	9.4 S	133.2 W	—	171	KH82-4-8	28.23 N	132.46 E	2630
90	CapHG33	10.57 S	130.29 W	4040	181	KH80-3-21	31.43 N	157.27 E	3950
91	CapBG30	17.28 S	160.59 W	4710	182	KH80-3-16	32.4 N	158.47 E	2450
92	CapBG6	10.5 S	170.03 E	—					
93	CapBG8	13.38 S	174.58 E	—					
94	CapBG24	19.28 S	173.44 W	—					
95	CapBG6	11 S	174 W	4390					
96	Dolphin1	12.1 S	144.25 W	4332					

Serial numbers for core samples correspond with those in Figure 1.

**Appendix 2.** Number of valves (shown as number of half-valves) and percent abundances of *Thalassionema* species and their morphological types out of the total *Thalassionema* counts.

Ser. No.	Sample name	<i>T. bacillare: Ba</i>	<i>T. bacillare: Ba (%)</i>	<i>T. bacillare: Bb</i>	<i>T. bacillare: Bb (%)</i>	<i>T. bacillare: Bh</i>	<i>T. bacillare: Bh (%)</i>	<i>T. frauenfeldii</i>	<i>T. frauenfeldii (%)</i>	<i>T. nitzschoides:</i> <i>Na+Nc (%)</i>	<i>T. nitzschoides:</i> <i>Na+Nc (%)</i>	<i>T. nitzschoides: Na</i>	<i>T. nitzschoides: Na (%)</i>	<i>T. nitzschoides: Ne</i>
1	MUK12BG							235	33	211	30	22		
2	TP40-1					7	6	30	28	18	17	7		
3	CK8							31	27	48	42			
4	USSR3357							24	24	25	25	1		
5	USSR3403	1	0			5	2	89	43	26	13			
6	USSR3274	4	3			8	6	69	50	10	7	9		
7	CK11					4	3	10	8	39	33	1		
8	USSR3257	15	3			10	2	115	26	198	45	5		
9	USSR3114	11	9			9	7	31	25	27	22	2		
11	USSR3109	10	4			7	3	61	22	116	42	10		
12	USSR3108	3	3			2	2	20	18	33	29	11		
13	CK13-3	1	1			1	1	10	6			61		
14	USSR3163	8	3			18	7	59	24	15	6	80		
15	CK4					1	0	5	2			78		
16	JYNII-10G	16	6	12	5	14	5	5	2	24	9	134		
17	JYNII-8G	5	2	12	5	12	5	3	1	5	2	143		
19	TP71	14	7			20	11	54	29	51	27	12		
20	JYNII-14G	12	2	24	4	51	8	39	6	38	6	289		
21	Takuyō6	5	2	9	4	22	9	35	14	55	22	10		
22	JYNII-17G	13	6	19	8	25	11	25	11	10	4	80		
23	USSR3449	36	20	30	17	9	5	7	4	37	21	35		
25	USSR3225	13	5	9	4	44	17	51	20	36	14	27		
26	JYNII-19	15	6	25	10	28	11	28	11	2	1	88		
28	CK16	3	1	66	30	3	1	2	1	1	0	113		
29	USSR4084	2	2	43	37	4	3					44		
30	TP97	17	8	5	2	17	8	15	7	1	0	131		
33	USSR3493	13	4	13	4	40	13	35	12	1	0	124		
37	Cap2BG1			3	2					1	1	156		
38	MukB10G					8	4	86	45	56	29			
46	Cas2					2	1	12	3	28	7	21		
47	Cusp9G							73	12	9	1	29		9
49	MukB31G											4		
52	USSR4183											93		
53	CK3			3	1	1	0					15		15
54	Cusp4G					2	1	2	1	38	5	23		
64	MP20-2	10	4	187	81					2	2	74		
68	Chub4	4	4	26	23							38		
69	Chub5	19	12	35	23	5	3							
71	ChubVIG	1	0					23	10			46		
73	ChubVII	5	2	1	0	4	2	40	18			38		
74	MSN150G	13	12	18	16					1	0	72		
75	ChubVIII											11		
76	DWBG6	2	1	6	4							59		
77	DWHT8	15	9	12	7							96		
78	MSN147G			4	3							97		
79	DWBG8	5	3	7	4							88		
80	Cap48BG1			3	1							180		
81	MSN142G	2	1	3	2							156		
82	MP11-1	1	0	2	1							203		
83	DWBG149	9	4	2	1							181		
84	DWBG12	2	1	4	2							141		
85	MSN141G	1	0	2	1							205		
86	DWBG13			1	0							196		
87	MSN136G	2	2	2	2							83		
88	DWHH89											204		
99	CapBG10-3	1	0	57	26							142		
100	CapBG15	6	3	45	23					3	1	129		
109	DWBG101											50		
112	DWBG108			11	5							47		
113	MSN100G											2		
114	MSN99G											4		
115	MSN97G													
118	DWBG64													
119	DWBG63													
120	DWBG61													
121	DWHG-36													
166	V21-84	3	2	1	1	16	8	6	3	4	1	151		
167	V21-83			29	9	11	3	5	2	4	1	240		

Serial numbers for core samples correspond with those in Figure 1

## Appendix 2. (Continued).

<i>T. nitzschoides: Ne (%)</i>	<i>T. nitzschoides: Nf (%)</i>	<i>T. nitzschoides: Ng (%)</i>	<i>T. nitzschoides: Nh (%)</i>	<i>T. nitzschoides: Ni (%)</i>	<i>T. nitzschoides: Nj (%)</i>	<i>T. pseudonitzschoides (%)</i>	<i>T. symediforme (%)</i>	<i>T. synediforme (%)</i>	<i>other Thalassionema species</i>	Total <i>Thalassionema</i> spp.
3						206	29		30	704
6						35	32	9	109	
0						33	29	2	114	
1						45	45	4	101	
0						81	39	2	206	
6	2	1				26	19	11	139	
1			1	1		63	53		118	
1						86	19	13	442	
2			2	2		43	34		125	
4						69	25	4	277	
10						36	32	1	112	
37	52	32	6	5		7	4	22	163	
32	2	1	9	6		47	19	1	247	
28	163	59	17	7		4	1	9	276	
50	12	5	16	6		37	14	12	266	
56	46	18	16	6		9	4	4	255	
6						32	17	4	187	
48	22	4	4	1		96	16	2	25	602
4			1	0		107	43	4	248	
34	8	3	15	6		35	15	3	233	
20			3	2		13	7	2	5	177
11			13	5		55	21	9	257	
36	8	3	18	7		33	13		245	
52	11	5	6	3		5	2	8	218	
38	2	2	7	6		5	4	8	115	
60	4	2	4	2		21	10	5	220	
42	2	1	18	6		31	10	2	18	297
91			8	5				1	2	171
						39	20	3	192	
5	86	22	161	41		74	19	10	394	
4	193	89	13	6				3	218	
5	164	27	254	41		74	12	11	614	
2	122	56	86	39		5	2	2	219	
41	92	41	27	12		5	2	4	225	
6	125	48	57	22		10	4	12	261	
10								5	230	
33	35	31	1	1		2	2	6	114	
48			1	1		9	6	11	154	
20	49	21	93	40		21	9		233	
17	51	22	53	23		24	11	12	228	
65	1	1	5	5		2	2		111	
4	130	51	87	34		15	6	12	256	
35	77	45	16	9				10	170	
56	21	12	4	2		1	1	21	170	
82	8	7	7	6		2	2		118	
55	45	28	9	6		1	1	4	159	
80	26	12	7	3				10	226	
91			2	1				8	171	
85			16	7		7	3	9	238	
90	6	3	2	1				1	201	
83	7	4	11	6				5	170	
87	9	4	14	6				5	236	
86	25	11	3	1				2	227	
81	5	5	10	10					102	
89	3	1	18	8		1		2	228	
64	6	3						17	223	
65								17	197	
18	152	55			14	5	4	55	278	
20	86	37			36	16	4	48	232	
1					17	8	178	2	204	
					20	10	85	5	205	
2					30	15	151	10	206	
					69	33	7	5	209	
2					348	81	68	133	427	
					187	76	24	64	1	
					171	79	30	13	245	
						14	16	7	217	
78	6	3	2	1				3	193	
73	23	7	4	1				12	328	

## References

- Akiba, F., 1882. Taxonomy and biostratigraphic significance of a new diatom, *Thalassionema schraderi*. *Bacillaria*, **5**: 43–61.
- Ansrews, G. W., 1976. Miocene marine diatoms from the Choptank Formation, Calvert County, Maryland. *U. S. Geological Survey Professional Paper*, **910**: 1–26.
- Baldauf, J. G. & J. A. Barron, 1991. Diatom biostratigraphy: Kerguelen Plateau and Prydz Bay region of the Southern Ocean. In: Barron, J. A., Larsen, B. et al. (Editors), Proceedings of the Ocean Drilling Program, Scientific Results, 119. Ocean Drilling Program, College Station, pp. 547–598.
- Baldauf, J. G. & A.-L. Monjanel, 1989. An Oligocene diatom biostratigraphy for the Labrador Sea: DSDP Site 11 and ODP Hole 647A. In: Srivasta, S. P., Arthur, M., Clement, B. et al. (Editors), Proceedings of the Ocean Drilling Program, Scientific Results, 105. Ocean Drilling Program, College Station, pp. 323–347.
- Barron, J. A., 1985. Late Eocene to Holocene diatom biostratigraphy of the equatorial Pacific Ocean, Deep Sea Drilling Project Leg 85. In: Mayer, L., Theyer, F., et al. (Editors), Initial Reports of the Deep Sea Drilling Project, 85. U. S. Government Printing Office, Washington D.C., pp. 413–456.
- Castracane, F., 1886. Report on the Diatomaceae collected by H. M. S. Challenger during the years 1873–1876. Report of the Scientific Results of the Voyage of H. M. S. Challenger 1873–1876, *Botany*, **2**: 1–178.
- Cleve-Euler, A., 1949. Littoral diatom from Tristan da Cunha. Results Norweg. Sci. Exp. to Tristan da Cunha 1937–1938, 18. Norske Videnskaps Akademi Publ, Oslo, pp. 1–30.
- Cleve, P. T. & A. Grunow, 1880. Beitrage zur Kenntniss der arctischen Diatomeen. *Kongliga Svenska Vetenskaps-Akademiens Handlingar*, **17**(2): 1–121.
- Fenner, J. & N. Mikkelsen, 1990. Eocene-Oligocene diatoms in the western Indian Ocean: taxonomy, stratigraphy and paleoecology. In: Dancan, R. A., Backman, J., Peterson, L. C. et al. (Editors), Proceedings of the Ocean Drilling Program, Scientific Results, 115. Ocean Drilling Program, College Station, pp. 433–463.
- Gladenkov, A. Y. & J. A. Barron, 1995. Oligocene and early Middle Miocene diatom biostratigraphy of hole 884B. In: Rea, D. K., Basov, I. A., R., Scholl, D. W. and Allan, J. F. (Editors), Proceedings of the Ocean Drilling Program, Scientific Results, 145. Ocean Drilling Program, College Station, pp. 21–41.
- Greville, R. K., 1865. Description of new genera and species from Hong Kong. *The Annals and magazine of Natural History Series III*, **16**: 1–7.
- Hallegraeff, G. M., 1986. Taxonomy and morphology of the marine plankton diatoms *Thalassionema* and *Thalassiothrix*. *Diatom Research*, **1**(1): 57–80.
- Hasle, G. R., 1960. Phytoplankton and ciliate species from the tropical Pacific. Skr. Norske Vidensk.-Akad., Oslo, *I Mat.-Nat. Kl.*, **2**: 1–50.
- Hasle, G. R., 1999. *Thalassionema synediforme* comb. nov. and *Thalassiothrix spathulata* sp. nov. two marine planktonic diatoms from warm waters. *Phycologia*, **38**: 54–59.
- Hasle, G. R., 2001. The marine, planktonic diatom family Thalassionemataceae: morphology, taxonomy and distribution. *Diatom Research*, **16**(1): 1–82.
- Hasle, G. R. & R. E. Mendiola, 1967. The fine structure of some *Thalassionema* and *Thalassiothrix* species. *Phycologia*, **6**(2/3): 107–125.
- Hasle, G. R. & E. E. Syvertsen, 1996. Marine diatoms. In: Tomas, C. R. (Editor), Identifying marine diatoms and dinoflagellates. Academic Press, San Diego, pp. 5–385.
- Heiden, H. & R. R. Kolbe, 1928. Die marinene Diatomeen der Deutschen Südpolar-Expedition 1901–1903. *Deutsche Südpolar-Expedition*, **8**(5): 447–715.
- Heurck, H. van, 1881. Synopsis des diatomees de Belgique. Atlas. Decauj et Cie, Anvers, pl. 31–77.
- Hustedt, F., 1958. Diatomeen aus der Antarktis und dem Südatlantik. *Deutsche Antarktische Expedition 1938/1939*, **11**: 105–191.
- Kanaya, T., 1959. Miocene diatom assemblages from the Onnagawa Formation and their distribution in the correlative formations in northeast Japan. *Sci. Rep. Tohoku University*, **2**<sup>nd</sup> Ser. (*Geol.*), **30**: 1–130, 11 pls.
- Kanaya, T. & I. Koizumi, 1966. Interpretation of diatom thanatocoenoses from the North Pacific applied to a study of core V20-130 (Studies of deep-sea core V20-130. Part IV). *Sci. Rep. Tohoku University*, **2**<sup>nd</sup> Ser. (*Geol.*), **37**(2): 89–130.
- Kawai, H., 1972. Hydrography of the Kuroshio Extent. In: Stommel, H., & Yosshida, K., (Editors), Kuroshio, its physical aspects, pp. 235–341.
- Kennett, J. P., G. Keller & M. S. Surinivasaon, 1985. Miocene planktonic foraminiferal biogeography and paleoceanographic development of the Indo-Pacific region. *Geol. Soc. America, Mem.*, **163**: 197–235.
- Kolbe, R. W., 1954. Diatoms from eqatorial Atlantic cores. *Reports of the Swedish Deep-Sea Expedition*, **6**(1): 1–49.
- Kolbe, R. W., 1955. Diatoms from eqatorial Atlantic cores. *Reports of the Swedish Deep-Sea Expedition*, **7**(3): 150–184.
- Meister, F., 1932. Kieselalgen aus Asien. Gebrüder Borntraeger, Berlin, pp. 1–56.
- Mereschkowsky, C., 1902. Les types de l'endochrome chez les Diatomées. *Scripta Botanica Horti Universitatis Petroplitanae*, **21**: 107–193.
- Moreno-Ruiz, J. L. & S. Licea, 1995. Observations on the valve morphology of *Thalassionema nitzschiooides*

- (Grunow) Hustedt. *In:* Marino, D. and Montresor, M. (Editors), Proceedings of the 13th International Diatom Symposium. Biopress, Bristol, pp. 393–413
- Norris, R., 2000. Pelagic species diversity, biogeography, and evolution. *Paleobiology, supplement to* **26**(4): 236–258.
- Pahnke, K. & R. Zahn, 2005. Southern hemisphere water mass conversion linked with North Atlantic climate variability. *Science*, **307**(5716): 1741–1746.
- Pantocsek, J., 1886. Beiträge zur Kenntnis der fossilen Bacillarien Ungarns. I. Nagy-Topolosany: J. Platzko, 30 pls.
- Peragallo, M., 1903. Le Catalogue général des Diatomées. Clermont-Ferrand, pp. 472–973.
- Sancetta, C., 1978. Neogene Pacific microfossils and paleoceanography. *Marine Micropaleontology*, **3**: 347–376.
- Sancetta, C. & S. Silvestri, 1986. Pliocene-Pleistocene evolution of the North Pacific ocean-atmosphere system, interpreted from fossil diatoms. *Paleoceanography*, **1**(2): 163–180.
- Schmitz, W. J., Jr., 1996. On the world ocean circulation, Vol. 1., some global features: North Atlantic circulation. Woods Hole Oceanographic Institution Technical Report WHOI-96-03: 1–141.
- Schrader, H.-J., 1973. Cenozoic diatom biostratigraphy from the northwest Pacific, Leg 18. *In:* Kulm, D. G., von Huene, R. *et al.* (Editors), Initial Reports of the Deep Sea Drilling Project, U. S. Government Printing Office, Washington D.C., pp. 673–797.
- Schrader, H.-J., 1978. Diatoms in DSDP Leg 41 sites. *In:* Lancelot, Y., Seibold, E. *et al.* (Editors), Initial Reports of the Deep Sea Drilling Project. U. S. Government Printing Office, Washington D.C., pp. 791–817.
- Schrader, H.-J. and R. Gersonde, 1978. Diatom and silicoflagellates. *In:* Zachariasse, W. J. *et al.* (Editors), Utrecht Micropaleontological Bulletins, pp. 129–176.
- Schuette, G. & H.-J. Schrader, 1982. *Thalassiothrix pseudonitzschioidea* sp. nov.: A common pinnate diatom from the Gulf of California. *Bacillaria*, **5**: 213–223.
- Simonsen, R., 1974. The diatom Plankton of the Indian Ocean Expedition of R/V “Meteor” 1964–1965. “Meteor” Forsch-Ergebnisse Reihe D, (19): 1–66.
- Simonsen, R., 1992. The diatom types of Heinrich Heiden in Heiden and Kolbe 1928. *Bibliotheca Diatomologica*, **24**: 1–99.
- Tanimura, Y., 1999. Varieties of a single cosmopolitan diatom species associated with surface water masses in the North Pacific. *Marine Micropaleontology*, **37**: 199–218.